1-1-2020

Solids velocity measurement using electric capacitance sensor assemblies

Usama Abrar

Liu Shi

Nasif Raza Jaffri

Qin Li

Hassan Raza Sindhu
Edith Cowan University

See next page for additional authors

10.1088/1757-899X/715/1/012097

Abrar, U., Shi, L., Jaffri, N. R., Li, Q., Sindhu, H. R., & Omar, M. W. (2020). Solids velocity measurement using electric capacitance sensor assemblies. In *IOP Conference Series: Materials Science and Engineering, 715*(1), Article 012097. https://doi.org/10.1088/1757-899X/715/1/012097

Solids velocity measurement using electric capacitance sensor assemblies

Solids velocity measurement using electric capacitance sensor assemblies

Usama Abrar[1,*], Liu Shi[1], Nasif Raza Jaffri[1], Qin Li[2], Hassan Raza Sindhu[3] and Mian Waqas Omar[4]

[1]School of Control and Computer Engineering North China Electric Power University Beijing 102206 China
[2]Institute of Mechanics Chinese Academy of Science Beijing 100190 China
[3]Department of Electrical Engineering Cowan University, Joondalup Perth Western Australia 6027
[4]Department of Computer Engineering Bahria University Islamabad Pakistan

*E-mail: uabrar@gmail.com

Abstract. This paper covers the application of the cross-correlation method for measuring the velocity of solid particles. Capacitive electrodes are used as primary sensors to measure the time required by the solid particles to cover a known distance between the electrodes. The capacitive variations of both the electrode sensors are stored in computer synchronously for offline estimation of the velocity of the solid particles. Single glass marble is used as a solid particle to conduct the performance in the lab for its good signal to noise ratio (SNR) and vivid graphs. Matlab R2018a is used as a programming tool to perform the cross-correlation algorithm. The distance between the sensors is adjusted optimally. The results were realistic to ensure the correctness of the system.

1. Introduction

Batch flow and continuous flow are two major techniques used to flow solid particles in industry. In the first one, the solid particles are divided into a number of bulks and are processed together, whereas the particles are processed without interruption in the later one. Their usage is varied from industry to industry and also depends upon the measuring and processing limitations [1]. In a variety of industrial processes, solid particles are dealt with the manner of batch flow. Feeding coal to the furnace is an important example of this technique, this can be done by using the conveyer belt but most of the times it is done pneumatically [2], [3]. Monitoring is the backbone of control part of the modern industry. In the absence of proper monitoring and control, it is impossible to achieve maximum efficiency from any industrial process and thus resource wastage takes place. Recently, the coal process industry has taken a few steps further by implying online monitoring, data logging and control of coal fed to the furnace by pneumatic means. Lately, there has been an emphasis on the precision and accuracy of these online measurements of solid particles flow. In these measurements, the parameters like flow rate, flow pattern, humidity, density and mass of the flowing solid are of main interests. There are other important notable parameters as well such as mass flow rate, pipeline erosion time that fundamentally depends upon the mass flow rate of the solid particles [4], [5]. A large number of techniques are available to measure the flow rate of solid particles depending upon sensing methods,

sensitivity, and technology used. Digital imaging, optical sensing, acoustic techniques, radiometric methods, electrostatic sensors, and capacitive sensors are the notable techniques used for the measurement of Gas/Solid particle flow rate measurement. In case of dilute concentration of solid particles acoustic technique, optical sensors, and digital imaging work better. But there are also some techniques that work better even in high concentration like radiometric method, however, there is a chance of radiation leakage which can be avoided by proper shielding [6], [7]. But if an economical, trustworthy, harmless and robust solution is required, the electrostatic and capacitive sensors are the best choices. Capacitance measurement method is extensively employed in online and offline assessments of flow parameters. The capacitive measurement method is economical, accurate, and robust. Moreover, it has non-invasive nature among the rest measurement techniques [8]. Despite the fact of being simple robust and dynamic in its response several factors try to adversely affect the system response thus inculcating errors - the multiphase complex and variable flow, non-uniform sensitivity distribution of the electrode pair, the deposition of the solid particles on the internal walls of the channel's area where the electrodes are attached- moisture, solid composition, particles size, and contents [9].

This paper covers the preliminary investigations on the velocity of the solid particles flowing through the channel using electric capacitance measurement and applying the algorithm of cross-correlation to calculate the time required by the particles to flow through the channel. This paper focuses on the time required to create similar variation patterns in the capacitance values as the dielectric flows through the channel. The flow of the solid particles is based upon the assumption that the particles are moving parallel to the axis of the pipe and perpendicular to the plane of the sensor such that every passing particle has to flow through both the sensors after an interval of time. For a known distance between the two sensors, the ratio between the distance and time to cover that distance shows the mean velocity of the solid particles flowing through the channel.

1.1. Pneumatic conveying

The Pneumatic Conveying (derived from 'Pneumatikós' depending upon wind or air) is a most commonly used technique of material transportation in the industry [10]. It is generally an automatic system and is based upon the phenomenon of transportation of solid particles –powdered or granular within a piping system along with gas/air stream. The transportation of solid particles is based upon the high, low or negative pressure of air/gas. The solid particles are separated from the air on arrival at the destination [11]. The schematic of the pneumatic conveying system is shown in figure 1.

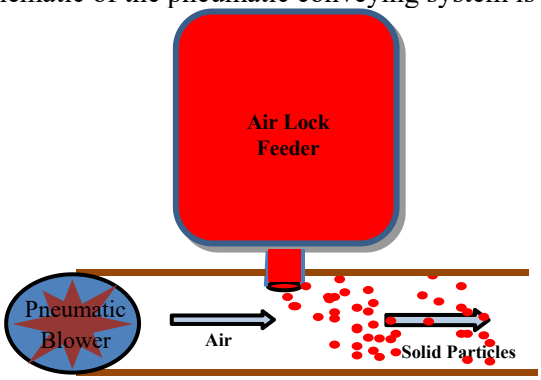

Figure 1. Pneumatic flow of solid particles.

The history of pneumatic conveying of the solids finds its traces in the era of ancient Greeks. Hero, a Greek Physicists, (10AD-85AD) gave the concept of Pneumatic Conveying [12]. The lead pipes for water transportation used by Romans and gas transportation bamboo tubes used by Chinese are from a prehistoric era. The granular solids transportation by the pneumatic system was introduced in 1920 [11]. This system was introduced in cement and coal industry in the1930s [13]. Since 1930-1960s remarkable efforts were done in the promotion and improvement of pneumatic conveying efficiency in

Japan, Germany, and USA [14]. Despite the fact that pneumatic conveying may cause damage to both pipes and particles and can transport to a limited distance while consuming high power [11], [15]. It is widely used in agricultural, chemical, mining food and mineral industry [16]. The reason is its ease of automation and control, dust-free transportation, low labor, and maintenance cost and last but not the least possibility of conveying of toxic and hazardous materials safely.

Solids are different from one another by their shapes, viscosity, density, stickiness, brittleness etc. Thus, various solids display different flow behaviors. Moisture content in the solid particles produces cohesive strength. The cohesiveness is also visible by temperature variation. Few solids are sensitive to rise in temperature. Others are reactant to a constant temperature. Cohesiveness is also dependent upon particle size. Finer powders are more cohesive also they have higher wall friction and thus difficult to flow smoothly [17]. If the solid particles are allowed to stay at rest for a longer time, the compaction loads due to head pressure can produce a strong cohesive bond. A chemical reaction, crystallization, or adhesive bonding can also cause this. Sometimes, after a cohesive arch is broken up, say by somehow initiating flow, the material can revert to its original flow condition and not exhibit a similar cohesion if left at rest again. On the other hand, some materials will time and again, bridge and rat-hole even after flow is re-initiated [18].

2. Mathematical description of velocity measurement

The velocity of the solid particles flowing through a channel can be computed using the cross-correlation technique [19]. Figure 2 elaborates the principle of calculating the velocity of solid particles using the cross-correlation technique. The cross-correlation of the two signals a(t) and b(t) is defined by equation 1

$$C(\tau) = \frac{1}{T}\int_0^T a(t)b(t+\tau)d\tau, \tag{1}$$

where $T \to \infty$.

Equation 1 shows the similarity between a(t) and b(t) while shifting b(t) along the time axis to $b(t+\tau)$. For a certain value of $\tau = \tau_{max}$ where $C(\tau)$ gives the maximum value, both a(t) and shifted b(t) are said to be most similar. If a(t) is considered as a signal from the first sensor while b(t) is considered as a signal from the second sensor. Since both the sensors are attached along the axis of the pipe in such a way that the solid particles flowing from the first sensor after a delay passes through the second sensor [20], the signals from both the sensors are the same with a difference of time delay which is the time required by the solid particles to flow from first sensor to the second sensor. If the distance between the sensors is obtained, the average velocity of the particles can be found by taking the fraction between the distance D and the time τ_{max}. In real time scenario the data is stored from both the sensors as discrete time values, so the cross-correlation of discrete time signals is defined by equation 2.

$$C[m] = \frac{1}{T}\sum_{n=0}^{T} a[n]b[n+m], \tag{2}$$

where $T \to \infty$.

However, it is impossible to find cross-correlation while extending $T \to \infty$. The modified version of cross-correlation is shown in equation 3.

$$C[m] = \frac{1}{L}\sum_{n=0}^{L} a[n]b[n+m], \tag{3}$$

where L is the length of the frame size, used to calculate the cross-correlation. It is the number of samples in a summation. m is the number of delayed samples-time delay [8]. In other words, L number of samples of $a[n]$ is multiplied by L number of samples of shifted $b[n+m]$. If Δt is the sampling interval, The time to obtain peak of the cross-correlation function is given by $\tau_{max} = m * \Delta t$. The average velocity of the solid particles is given by equation 4.

$$V = D/\tau_{max} \ . \tag{4}$$

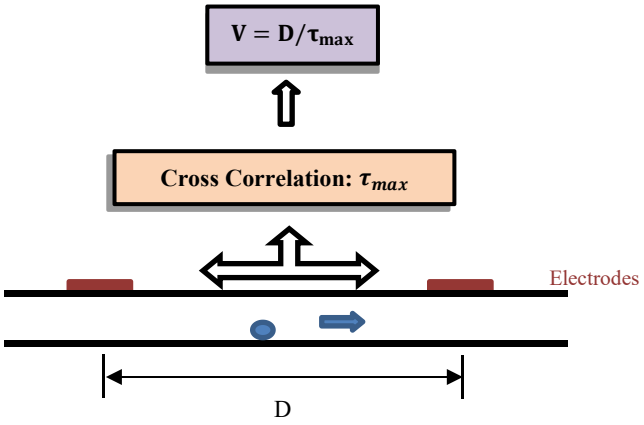

Figure 2. Velocity of solid particles using cross correlations.

The choice of the suitable distance between the two sensors is important. If the sensors are placed at a farther distance, the slow data acquisition rate may occur [21]. However, the better similarity between the signals is possible if the distance between the sensors is small. Although there is a chance of cross-interference of the signals of the two sensors if they are very close to each other. So the distance between the sensors is chosen depending upon the similarity of the signals and the dynamic behaviour of the system [4], [22].

3. Experimental setup

An Electric Capacitance Assembly system consists of three main components: the sensor, the data acquisition circuit, and the computer. The sensor is a single or more pair of metallic electrodes. The size, shape and the mutual distance between the pairs and among the electrodes of the individual pair are adjustable as per requirements. These electrodes are mounted on the insulated pipe which is extraneously covered with an earthed metallic sheet. The data acquisition circuit: typically excite the capacitive electrode pairs and converts the capacitance into the voltage which is conditioned and digitized for data acquisition. The computer stores and analyses the data by applying different mathematical techniques [22].

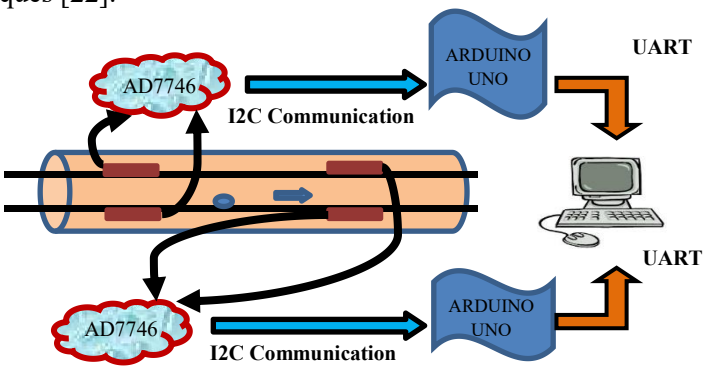

Figure 3. Block diagram of experimental setup.

The block diagram of the experimental setup is shown in figure 3. The glass marble flows through a rectangular, insulated and inclined channel- fixed on a stand and the angle of inclination can be varied as per requirements. The dimensions of the channel are 1×2×60 cm^3. Two pairs of electrodes 'Sensor 1' and 'Sensor 2' of dimensions 2×1 cm^2 and 1×1 cm^2 respectively are fixed on the lower and upper surface of the channel 16.7 cm (distance between their centers) apart such that the glass marble flowing through 'sensor 1' must flow through 'sensor 2'. The channel is enclosed in a metallic

shielding attached to a common ground with protective metallic shielding attached at the upper and lower ends of both the sensors to minimize the effects of the noise signals.

Eval-AD7746EBZ is a capacitance to digital converter evaluation board which is primarily used as data acquisition circuit for the measurement of capacitance between the electrodes. The main significance of AD7746 is its high resolution of 24-bits down up to 4aF and accuracy up to 4fF. Its full-scale capacitance rage is ±4pF. The maximum sampling rate of the device is 90Hz. The capacitance to be measured is directly connected to its terminals- Excitation terminal and Input terminal. It communicates through the I2C interface with microcontroller (Arduino-UNO). The registers were configured according to the Data Sheet for single mode capacitance measurement using I2C communication protocol. The raw data from AD7746 is received by Arduino and sent to the Computer through UART where the values were fed in the formula to compute the capacitance of both the sensors. The computer-program also gives the desired sampling interval to the Microcontroller that starts dropping off the data and thus stores at the required sampling rate [23]. The flow diagram of the data acquisition and storage is shown in figure 4.

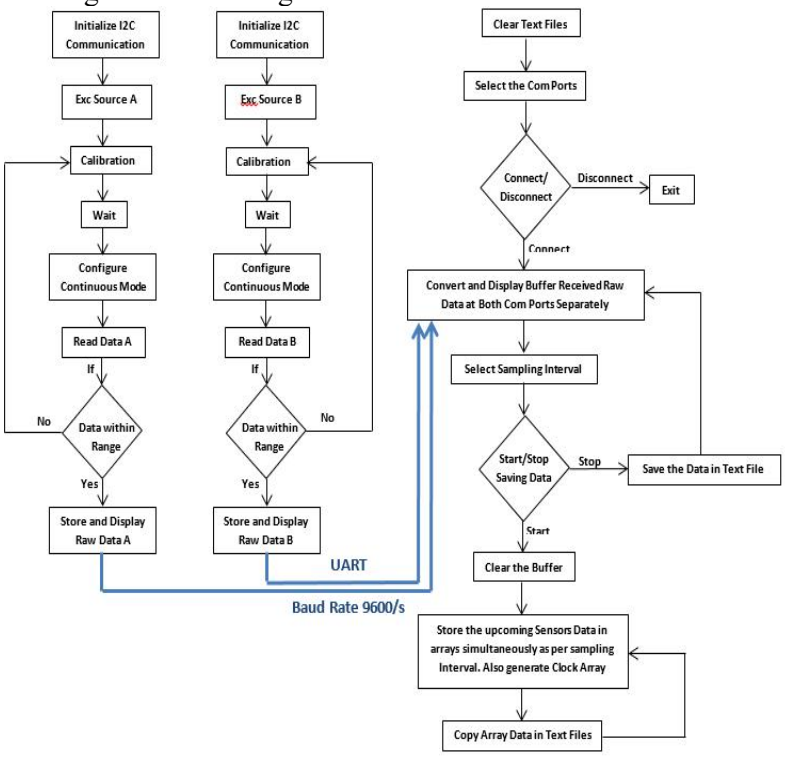

Figure 4. Flow diagram for data acquisition and data storage.

The data obtained from the microcontroller through UART at a baud rate of 9600/s is displayed on the GUI. The sampling interval is adjusted and as the command is given for data storage, it clears the buffer, generates a time clock variable and then starts storing the next upcoming data according to the set time interval. The intermediate samples are discarded and not stored in respective arrays thus ensuring time synchronized data storage from both the sensors. The arrays are then stored in respective files for further processing.

4. Results and discussions

Figure 5 shows the capacitance values of sensor 1 and Sensor 2 as a single spherical glass marble of size 7 mm is allowed to flow through the channel. The sampling interval of 10 ms is adjusted for the record of data. The spikes in both the signals indicate the instants as the glass marble flows through the sensors respectively. The separation between the pair of the electrodes of individual sensor is approximately 1 cm (outer diameter of the pipe). The marble behaves as a dynamically flowing

dielectric medium between the electrodes of the sensor. The nature of the material (glass) and its size comparative to the diameter of the channel (space between the electrodes) is believed to give good signal to noise ratio. During the time glass marble has not reached the sensor 1, its capacitance value remains close to 0.4764 pF as the glass marble reaches the region of capacitance field, a sudden rise in the graph of sensor 1 is observed, the glass marble rolls down towards sensor 2 who until now has an average value maintained around 0.3128 pF the slight variations in both the signals are because of the noise that can be reduced by subtracting the average value of the signal from individual stored sample of the data. The difference in the average value of both the sensors is because of the size of the electrodes for both the sensors. Since sensor 1 is double in size as compared to sensor 2. However the variation in the average value of the capacitance for both the sensors is 0.1636 pF (52.3%). Also the spike of sensor 1 is wide in the initial then the graph sharpens suddenly. This is because in the design of sensor 1.

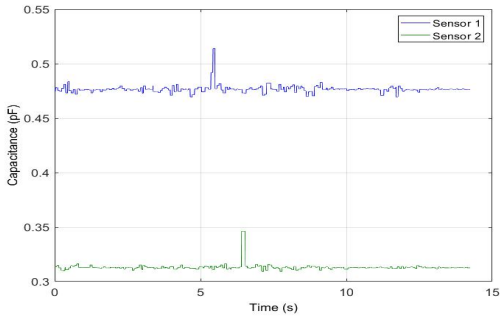

Figure 5. Output signals of capacitive sensors when the distance is 16.7 cm.

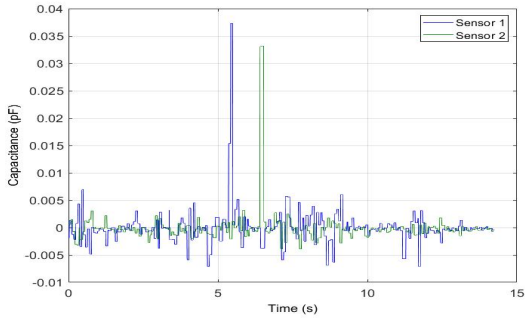

Figure 6. Output signals of both the sensors after noise reduction.

Two pieces of metal of approximate size 1x1cm^2 are placed over lapping each other which shows abnormality in the shape of the spike. However Sensor 2 electrode is a pair of single piece. The time is recorded for the flow of the glass marble through both the sensors. Figure 6 shows the normalized output of both the sensors after the noise reduction by subtracting the average value from individual signals.

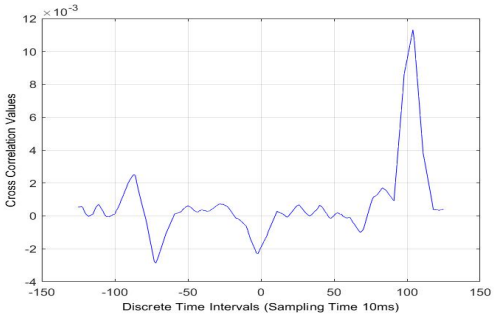

Figure 7. Typical cross correlation between the two sensors when the distance between them is 16.7 cm.

The cross-correlation is performed on the output signals of both sensors. Maltab R2018a is used to compute the cross correlation between the signals using equation 3. A window size of 125 discrete samples is used to compute cross correlation between the signals. Figure 7 shows the output of the cross correlation curve. Where maximum peak of the curve is obtained at 104th discrete time interval. This means that on shifting the window samples of Sensor 2 by discrete steps of 10 ms each it is 104th instant where both the curves match the most in their pattern. The pattern trend relies on the instant as glass marble flows through the sensor. So the peak of curve in figure 7 indicate the time required by the rolling glass marble to flow from sensor 1 to sensor 2 in discrete intervals. The separation between the two sensors is chosen as the distance between the centers of the electrodes of both the sensors which are 16.7 cm. The total time required by the glass marble to flow between Sensor 1 and Sensor 2 is 1.04 s. The velocity of the marble is found to be 0.16 m/s. Table 1 shows different iterations to calculate the velocity of the glass marble through the channel. The average velocity of the glass marble slowly rolling along a constant inclined surface is found to be 0.15 m/s.

Table 1. Velocity of glass marble using cross correlation.

Sr. No	Time Estimated (s)	Distance Between the Sensors (cm)	Velocity Estimated (m/s)
1	1.04	16.7	0.16
2	1.18	16.7	0.14
3	1.09	16.7	0.15

4.1. Limitations of the sensor

Table 2 shows the limitation of the sensor designed that is how fast moving solid particle can be detected by this sensor. Several iterations were performed on free rolling glass marble along the inclined surface.

Table 2. Effect of angle of inclination of channel on velocity of rolling solids.

Sr. No	Angle(θ˚)	Distance Between the Sensors(cm)	Time (s)	Velocity (m/s)
1	6.87	16.7	1.64	0.101
2	8.84	16.7	0.350	0.477
3	10.58	16.7	0.330	0.506
4	11.83	16.7	0.320	0.521
5	14.85	16.7	0.250	0.668
6	18.69	16.7	0.160	1.043

At horizontal surface where angle of inclination was θ˚ =0 there was no rolling in the glass marble. The rolling in the glass marble started when the angle of inclination was increased and on further increase resulted in the increase in the velocity of the glass marble. The reason is in the absence of forced response-when no input force is exerted on the marble, the only driving force is the rectangular component of gravity force acting along the plane of inclined channel. The magnitude of this force linearly increases as Cosine function of the angle of inclination acting along the plane of channel.

Keeping sampling interval fixed at 10 ms for data collection from AD7746 whose maximum output sampling rate as per data sheet is 90 samples/sec, the maximum velocity that can be computed by this capacitive sensor is 1.043 m/s. In the absence of the external force applied such velocity can be achieved as the angle of inclination of the channel is increased up to θ˚=18.69˚ As the angle is further increased. The value of m from equation 3 becomes gradually 0. i.e. not computable by the sensor for its limitations of sampling. Reason is solid particle is flowing through the distance D of equation 4 faster than the sampling frequency. Further higher velocity can be found either by using a higher frequency capacitance data acquisition circuit or by changing the dimensions of the sensors. Figure 8 shows the relationship between the velocity and angle of inclination of the channel.

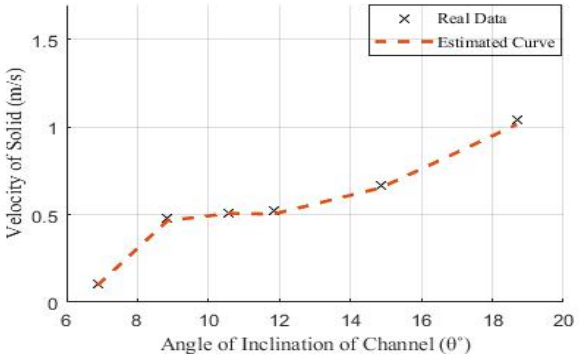

Figure 8. Effect of inclination of channel on the velocity of the solid.

$$V(\theta) = -0.0004354\theta^4 + 0.02364\theta^3 - 0.4634\theta^2 + 3.926\theta - 11.7 \quad (5)$$

Using curve fit tool and data from table 2, the relationship between the velocity of the glass marble and the angle of inclination is shown in equation 5.

5. Conclusion

An instrumentation system based upon the capacitance sensors has been developed in this paper. Experiments have been carried out on a rectangular channel. The results demonstrated that the average velocity of the glass marble was 0.15 m/s. This shows that the system is capable of data acquisition and offline measurement of the velocity of the particles. The instrumentation system is designed based upon AD7746 Evaluation Board and the microcontroller which can be installed in the industrial environment to provide particle flow parameters to system control units. In future, the system will be used to evaluate the performance of the instrumentation system on a dense phase pneumatic conveyor of pulverized fuel particles.

Acknowledgments

The authors wish to extend their gratitude to NSFC for sponsoring the research (No 61571189, 61871181) and to the State Administration of Foreign Experts Affairs for supporting the 111 project (ref: B13009).

References

[1] T. R. Dias, W. R. Melchert, M. Y. Kamogawa, F. R. P. Rocha, and E. A. G. Zagatto, “Fluidized particles in flow analysis: potentialities, limitations and applications,” Talanta, vol. 184, no. December 2017, pp. 325–331, 2018.

[2] J. wei Zhou, C. long Du, and Z. ling Ma, “Influence of swirling intensity on lump coal particle pickup velocity in pneumatic conveying,” Powder Technol., vol. 339, pp. 470–78, 2018.

[3] H. Lu, X. Guo, P. Li, K. Liu, and X. Gong, “Design optimization of a venturi tube geometry in dense-phase pneumatic conveying of pulverized coal for entrained-flow gasification,” Chem. Eng. Res. Des., vol. 120, pp. 208–17, 2017.

[4] H. Seraj, M. F. Rahmat, and M. Khalid, “Measurement of velocity of solid/air two phase fluid using electrostatic sensors and cross correlation technique,” Sci. Iran., vol. 20, no. 3, pp. 786–92, 2013.

[5] S. M. Rao, K. Zhu, C. H. Wang, and S. Sundaresan, “Electrical capacitance tomography measurements on the pneumatic conveying of solids,” Ind. Eng. Chem. Res., vol. 40, no. 20, pp. 4216–26, 2001.

[6] C. Hartmann, J. Wang, D. Opristescu, and W. Volk, “Implementation and evaluation of optical flow methods for two-dimensional deformation measurement in comparison to digital image correlation,” Opt. Lasers Eng., vol. 107, no. September 2017, pp. 127–41, 2018.

[7] M. B. Lima, S. I. E. Andrade, I. S. Barreto, L. F. Almeida, and M. C. U. Araújo, “A digital

image-based micro-flow-batch analyzer," Microchem. J., vol. 106, pp. 238–43, 2013.
[8] W. Zhang, C. Wang, W. Yang, and C. H. Wang, "Application of electrical capacitance tomography in particulate process measurement - A review," Adv. Powder Technol., vol. 25, no. 1, pp. 174–88, 2014.
[9] H. Q. Che, M. Wu, J. M. Ye, W. Q. Yang, and H. G. Wang, "Monitoring a lab-scale wurster type fluidized bed process by electrical capacitance tomography," Flow Meas. Instrum., vol. 62, no. September 2017, pp. 223–34, 2018.
[10] K. Malone and H. W. Fowler, A Dictionary of Modern English Usage., 2nd Editio., vol. 42, no. 3. Oxford University Press, 1983.
[11] G. E. Klinzing, "A review of pneumatic conveying status, advances and projections," Powder Technol., vol. 333, pp. 78–90, 2018.
[12] E. Papadopoulos, "Heron of Alexandria (c. 10–85 AD)," in Distinguished Figures in Mechanism and Machine Science, Dordrecht: Springer Netherlands, 2007, pp. 217–45.
[13] C. Ratnayake, "A Comprehensive Scaling Up Technique for Pneumatic Transport Systems," The Norwegian University of Sceince and Technology (NTNU), 2005.
[14] G. E. Klinzing, "Historical review of pneumatic conveying," KONA Powder Part. J., vol. 2018, no. 35, pp. 150–59, 2018.
[15] L. Cai, X. Pan, C. Xiaoping, and Z. Changsui, "Flow characteristics and stability of dense-phase pneumatic conveying of pulverized coal under high pressure," Exp. Therm. Fluid Sci., vol. 41, pp. 149–57, 2012.
[16] V. Mills, David. Jones, Mark. Agarwal, "Pneumatic Conveying of Coal and Ash," in Handbook of Pneumatic Conveying Engineering / Edition 1, 2004, pp. 170–208.
[17] W. Chen and A. W. Roberts, "A modified flowability classification model for moist and cohesive bulk solids," Powder Technol., vol. 325, pp. 639–650, 2018.
[18] H. Lu, X. Guo, Y. Jin, and X. Gong, "Effect of moisture on flowability of pulverized coal," Chem. Eng. Res. Des., vol. 133, pp. 326–34, 2018.
[19] M. O. Agolom, G. Lucas, and R. O. Webilor, "Measurement of velocity profiles in transient single and multiphase flows using inductive flow tomography," Flow Meas. Instrum., vol. 62, no. June 2017, pp. 246–54, 2018.
[20] X. Li, A. J. Jaworski, and X. Mao, "Comparative study of two non-intrusive measurement methods for bubbling gas-solids fluidized beds: Electrical capacitance tomography and pressure fluctuations," Flow Meas. Instrum., vol. 62, no. May 2017, pp. 255–68, 2018.
[21] K. Grudzień, Z. Chaniecki, and L. Babout, "Study of granular flow in silo based on electrical capacitance tomography and optical imaging," Flow Meas. Instrum., vol. 62, no. September 2017, pp. 186–95, 2018.
[22] M. Sun, S. Liu, J. Lei, and Z. Li, "Mass flow measurement of pneumatically conveyed solids using electrical capacitance tomography," Meas. Sci. Technol., vol. 19, no. 4, 2008.
[23] Z. Huang, J. Zhu, and L. Lu, "An AD7746-Based Data Acquisition System for Capacitive Pressure Sensor in Weather Detection Application," Key Eng. Mater., vol. 483, pp. 461–64, Jun. 2011.